A workspace evaluation of an eclipse robot
Marco Ceccarelli and Erika Ottaviano

Laboratory of Robotics and Mechatronics, DiMSAT, Università di Cassino, Via Di Biasio 43, 03043 Cassino, (Fr), Italy
E-mail: ceccarelli/ottaviano@ing.unicas.it

SUMMARY
In this paper we have proposed a numerical procedure for determining and evaluating the workspace of the eclipse robot architecture. The eclipse robot is a novel parallel architecture, which has been conceived and designed at the National Seoul University, Korea. The Eclipse robot design has been characterized in term of workspace characteristics, and optimum design solutions have been investigated as functions of the effect of design parameters on workspace.

KEYWORDS: Robotics; Design; Parallel manipulators; Workspace

1. INTRODUCTION

In the last two decades several parallel architectures have been designed following the success of the Stewart-Gough Platform. The main characteristics and advantages, with respect to open-chain manipulators, are recognized as greater stiffness, better accuracy and larger payload. Usually, the biggest limitation concerns the workspace.

The determination of the workspace of parallel architectures is an important issue, which has been addressed by few researchers. Procedures for workspace evaluation of parallel manipulators have been formulated by determining extreme paths;[1] computing conditions occurring at the workspace boundaries;[2] or formulating *ad-hoc* closed-form expressions for specific architecture, as for example in reference [3].

A novel 6-degrees of freedom parallel architecture, termed Eclipse, has been designed at the National Seoul University, Korea,[4,5] with the aim to overcome the workspace limitation and apply it to multi-face machining.[5]

In this paper we have proposed a procedure for the numerical determination of the Orientation and Position Workspace of the Eclipse parallel architecture. The Position Workspace is a set of reachable positions by a reference point in a Cartesian coordinate frame, it gives the positioning capability of a robot. The orientation workspace is the set of reachable orientations by the extremity link, namely the mobile plate, in terms of orientation angles, and it gives the orientating capability of a robot.

A specific algorithm has been formulated by taking into account the specific design of the Eclipse robot architecture in order to obtain a numerical procedure that has been useful for a parametric study of the effect of design parameters on workspace characteristics.

Preliminary results of workspace characterization of the eclipse have been presented in reference [6] and discussed in term of a unit workspace volume that has been recognized as a basic manifold for generating the workspace of an Eclipse robot.

2. KINEMATIC CHAIN AND PROTOTYPE OF ECLIPSE ROBOT

The kinematic chain of Eclipse robot architecture is shown in Fig. 1.

The Eclipse parallel architecture consists of three PRS serial sub-chains that move independently on a fixed circular guide. The letters P, R and S denote prismatic, revolute and spherical joints, respectively. Each leg can be actuated on the prismatic joints along the circular guide and vertical axis. The three legs can slide along the same circular guide. Each leg is connected to the mobile plate at the connection point H_k (k = 1, 2, 3) by means of a spherical joint. The Eclipse robot has 6 degrees of freedom, which are actuated through the 6 prismatic joints.

In order to describe the motion capability of an Eclipse robot a fixed frame XYZ has been fixed in the base frame with the origin at the center of the figure, Z-axis lying on a vertical direction and the X and Y axes being in a horizontal plane, as shown in Fig. 1. A moving frame xyz has been fixed in the moving plate with the origin coinciding with the operation point H, which is the center of the figure of the mobile plate. The z-axis is orthogonal to the plane of the moving plate; the x-axis has been fixed along the direction
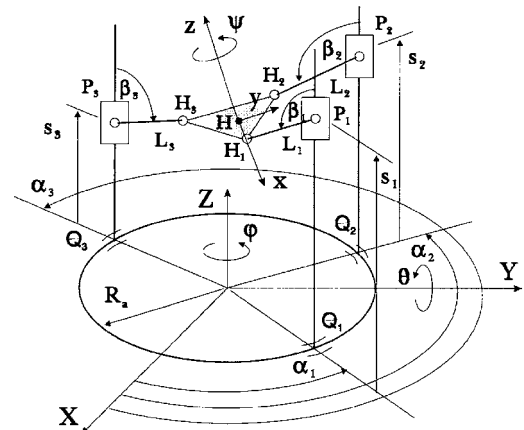
Fig. 1. Kinematic chain and parameters of an Eclipse robot architecture.

joining H to H_1; the y-axis is chosen in order to have a Cartesian frame.

The design parameters of the Eclipse chain are reported in Fig. 1 and they are:

- R_a, which is the radius of the circular guide on the fixed plate;
- α_k, which is the angle about Z-axis giving the position of the k-prismatic joint at point Q_k along the circular guide;
- s_k, which is the stroke giving the position of the k-prismatic joint at point P_k along the vertical axis of the prismatic guide;
- L_k, which is the size of the k-connecting rod from the prismatic guide to the movable plate;
- β_k, which is the joint angle of the k-revolute joint that is installed on the prismatic joint sliding on the vertical guide.

The size of the mobile plate is given by the size of the equilateral triangle $H_1H_2H_3$ and can be represented by HH_1.

The position of the operation point H can be described by its coordinates X, Y and Z, with respect to the XYZ frame. The orientation of the mobile plate has been represented in Fig. 1 by using the Euler angles φ, θ and ψ. The φ angle describes a rotation about Z-axis; θ describes rotation about Y-axis; and ψ describes a rotation about the moving axis z.

Hence, the workspace capability of the eclipse robot can be computed by determining all the positions and orienta-

Fig. 2. A built prototype of an Eclipse robot as 5-face machine in Seoul.[6]
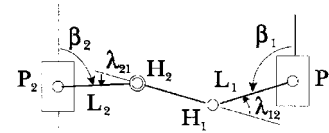
Fig. 3. A RSSR sub-mechanism for the evaluation of a reachable configuration of Eclipse.

tions reached by H and the mobile plate, respectively, when the input actuated joints are moved within an *a-priori* prescribed mobility range.

The kinematic variables for the eclipse robot are the input angles α_k and strokes σ_k of the prismatic joints. Angles β_k are passive joint variables, which determine the actual configuration of the mobile plate.

A prototype machine with an Eclipse robot architecture has been built as capable of machining plastic stock in Seoul,[5] and it is shown in Fig. 2. A spindle can be attached to the mobile plate and, because of a proper site of the mechanical design, it can move continuously from the vertical to the horizontal direction, and it can also rotate 360 deg. about z-axis. This motion capability is essential for 5-face machining.

The sizes of the design parameters for the built prototype of Fig. 2 are: R_a, which is equal to 300 mm; HH_1 is 100 mm; L_k is equal to 330 mm; the joint angles α_k have a range larger than a full rotation but for computational purposes they can be conveniently considered as 0–360 deg.; the strokes s_k are with the range of $(-300, 0)$, $(0, 200)$, $(0, 200)$, respectively. The practical values for α_k are related to the vertical guides being distant from each other at least 30 deg. The mobility of the three spherical joints is limited within a range of 60 deg., whose zero reference axis is located at an angle λ_k of 10 deg, -37 deg., and -37 deg, respectively, for the joints. The range of mobility of β_k is 0-180 deg.

3. A FORMULATION FOR WORKSPACE ANALYSIS AND EVALUATION

Workspace analysis is a specific problem in Direct Kinematics and it can be conveniently solved by formulating input-output equations in a suitable form for an easy repetitive calculations, which are needed to compute all the reachable positions and orientations of the mobile plate.

In the case of the Eclipse robot architecture one can base the formulation on the scheme of Fig. 3, which describes the RSSR sub-mechanism. This sub-mechanism is identified in the Eclipse robot architecture by using three connecting
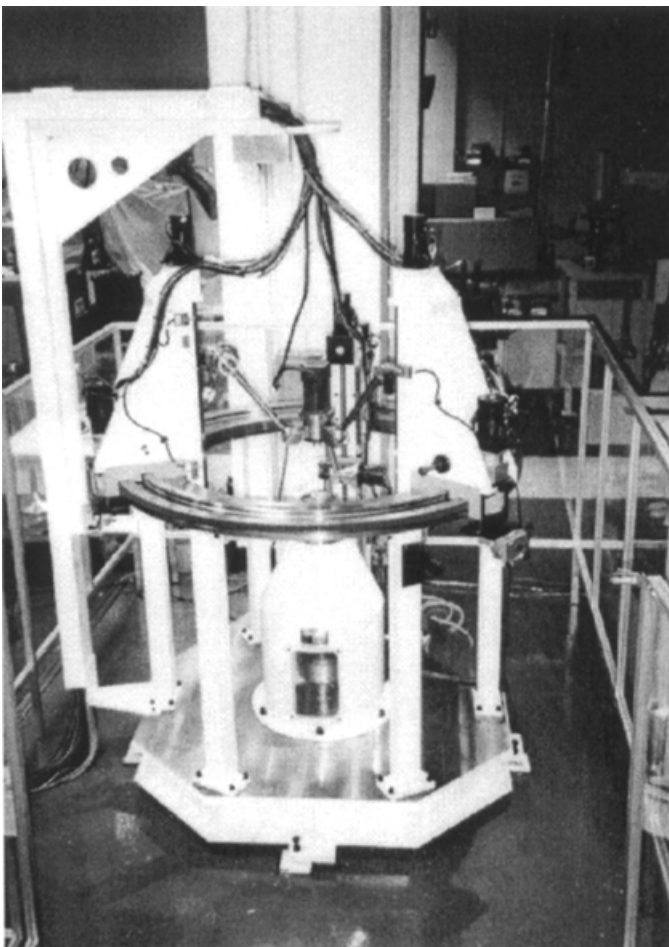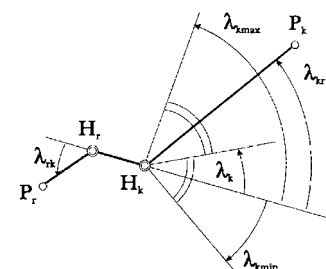
Fig. 4. A scheme for computing mobility constraint on joint angles of spherical joints.

Table I. Numerical procedure for workspace determination of the Eclipse robot architecture.
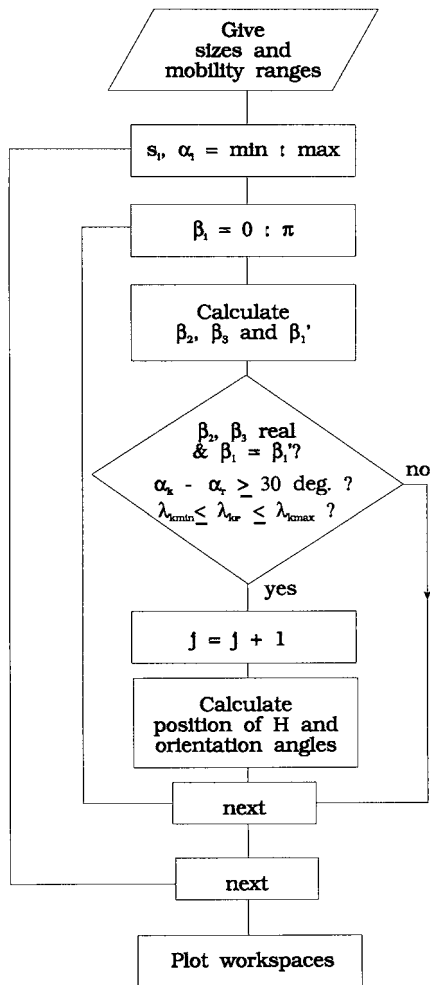
rods, as shown in Fig. 3, so that one will identify the RSSR mechanism in the parallel architecture by going from one point P_i to the neighbor one P_k. The output value β_k at P_k that one obtains as output from a RSSR sub-mechanism can be considered as the input for the next RSSR sub-mechanism.

In particular, assuming j input values α_{kj} and s_{kj} ($k=1,2,3$), from the geometry of Figs. 1 and 3 the j position and orientation of the Eclipse mobile plate can be computed
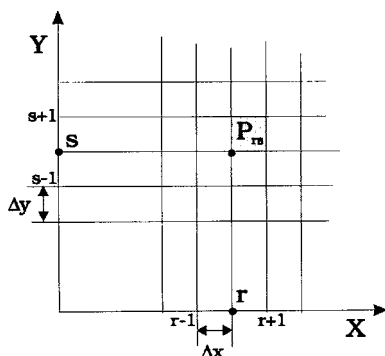
Fig. 5. A scheme for binary representation of a cross-section of a computed workspace.

as functions of the H coordinates and Euler angles, respectively, in the form:

$$X_j=\frac{x_{1j}+x_{2j}+x_{3j}}{3}; \quad Y_j=\frac{y_{1j}+y_{2j}+y_{3j}}{3}; \quad Z_j=\frac{z_{1j}+z_{2j}+z_{3j}}{3}; \quad (1)$$

$$\tan \varphi_j=\frac{y_{1j}-y_j}{x_{1j}-X_j}; \quad \tan \theta_j=\frac{z_{1j}-Z_j}{x_{1j}-X_j}; \quad \tan \psi_j=\frac{y_{1j}}{x_{1j}}; \quad (2)$$

where x_{kj}, y_{kj} and z_{kj} are the coordinates of the connecting point H_k, which are given by

$$x_{kj}=(R_a+L_k\sin\beta_{kj})\cos\alpha_{kj}; \quad y_{kj}=(R_a+L_k\sin\beta_{kj})\sin\alpha_{kj};$$
$$z_{kj}=s_{kj}+L_k\cos\beta_{kj}; \quad (3)$$

When $\theta=0$ occurs, no distinction exists between φ and ψ so that one can compute them from

$$\tan(\varphi_j+\psi_j)=\frac{y_{1j}-Y_j}{x_{1j}-X_j}; \quad (4)$$

but considering those proper values can be chosen in order to obtain continuous functions of the φ and ψ with previous and subsequent calculations. The angle β_{kj} can be calculated by using closure equations for RSSR sub-mechanism in a suitable procedure to determine a reachable configuration of the Eclipse architecture.

Referring to Fig. 3, the condition $H_iH_k=$constant can be expressed by using the coordinates of the connecting points H_i and H_k from the mechanism closure equations. After some algebraic manipulation one can obtain the input-output expression for the j configuration of Eclipse robot architecture in the form

$$A_{ij} \sin \beta_{kj}+B_{kj} \cos \beta_{kj}+C_{ij}=0 \quad (5)$$

where

$$A_{ij}= k_{4ij} \sin \beta_{ij}$$
$$B_{ij}=2(s_{ij}-s_{kj})L_i-2L_iL_k \cos \beta_{ij}$$
$$C_{ij}=k_{1ij}^2-H_iH_k^2+2(s_{ij}-s_{kj})L_i \cos \beta_{ij}=k_{3ij} \sin \beta_{ij} \quad (6)$$

with

$$k_{ij}=2R_a^2L_i(1-\sin(\alpha_i+\alpha_k))+L_i^2+L_k^s+(s_{kj}-s_{ij})^2$$
$$k_{2ij}=2L_iL_k \sin(\alpha_i+\alpha_k)$$
$$k_{3ij}=2R_aL_i(1-\sin(\alpha_i+\alpha_k))$$
$$k_{4ij}=2R_aL_i(1-\sin(\alpha_i+\alpha_k)) \quad (7)$$

By using Eqs. (5) and (7) β_{kj} angle is obtained as

$$\beta_{kj}=\tan^{-1}\frac{A_{ij}+\text{sgn}_k \sqrt{A_{ij}^2-B_{ij}^2-C_{ij}^2}}{B_{ij}+C_{ij}} \quad (8)$$

when the sign ambiguity is solved by inspecting the assembly configuration for congruence. In particular, the Eclipse prototype of Fig. 2 is described by $\text{sgn}_1=-1$; $\text{sgn}_2=1$ and $\text{sgn}_3=1$.

A configuration of the Eclipse robot architecture can be determined when α_{kj} and s_{kj} (k = 1,2,3) are given and β_{1j} is assumed so that β_{2j} and β_{3j} can be computed as congruent with β_{1j}. Numerically it can be easily obtained by computing β_{kj} with propersign in Eq.(8) so that this ensures the closure of the RSSR sub-mechanism loop. One can determine all the reachable configurations of Eclipse robot by scanning the mobility range of β_{1j}, β_{2j} and β_{3j} under the above mentioned congruence condition in agreement with the following kinematic constraints.

The above-mentioned numerical values of practical mechanical design of the prototype can be considered as kinematic constraints on the mobility of the joints.

In particular, the input joints can be given with the conditions

$$\alpha_k - \alpha_j \geq 30 \text{ deg} \tag{9}$$

$$\lambda_{kmin} \leq \lambda_{kr} \leq \lambda_{kmax} \tag{10}$$

in which

$$\lambda_{kmin} = \lambda_k - 60 \text{ deg}; \quad \lambda_{kmax} = \lambda_k - 60 \text{ deg}; \tag{11}$$

Angles λ_{kr} can be computed from the RSSR sub-mechanism of Fig. 3 by using the scheme of Fig. 4 to obtain

$$\lambda_{kr} = \pi - \cos^{-1}[(\mathbf{H_kH_r} \cdot \mathbf{H_kP_k}) / (H_kH_r \, H_kP_k)] \tag{12}$$

in which "•" is dot product between the vectors $\mathbf{H_kH_r}$ and $\mathbf{H_kP_k}$ that have the components given by the components of position vector of the corresponding points in the form

$$\mathbf{H_kH_r} \equiv (x_r - x_k; \, y_r - y_k; \, z_r - z_k);$$

$$\mathbf{H_kP_k} \equiv (u_r - x_k; \, v_r - y_k; \, w_r - z_k); \tag{13}$$

A numerical procedure for the workspace determination of Eclipse robot has been formulated as summarized in the flowchart of Table I. The angle β_1 is the angle computed as output in the RSSR sub-mechanism between P_3 and P_1 and it is compared with the given value β_1 in the scanning process with the aim to verify the closure of the parallel chain of Eclipse architecture by using the three RSSR sub-mechanisms among P_1, P_2, and P_3.

A numerical evaluation of the workspace can be deduced by formulating a suitable binary representation of a cross-section with a suitable scanning of the computed reached positions and orientations.

A binary matrix P_{rs} can be defined for a cross-section of the workspace as follows: If the (r, s) grid pixel includes a reachable point, then $P_{rs} = 1$; otherwise $P_{rs} = 0$, as shown in Fig. 5. For example, one can consider a cross-section at a given value of Z-Coordinate, then a point in the grid is indicated as P_{rs}, with r along X axis and s along the Y axis, namely,

$$r = \left[\frac{x + \Delta x}{x}\right]; \quad r = \left[\frac{y + \Delta y}{y}\right]; \tag{14}$$

where r and s are integers. Therefore, the binary mapping for th workspace cross-section is given by

$$P_{rs} = \begin{cases} 0 & \text{if} \quad P_{rs} \notin W(H) \\ 1 & \text{if} \quad P_{rs} \in W(H) \end{cases} \tag{15}$$

where W(H) indicates a workspace region; $\in$ stands for "belong to" and $\notin$ is for "not belonging to".

In addition, whilst scanning the vector of the computed reached positions to build P_{rs} through Eq. (15), it is possible to evaluate the dexterity performance of a manipulator by counting the times that each P_{rs} is reached.

Thus a suitable reach frequency matrix f_{rs} can be defined during the scanning process for P_{rs} with the condition for each entry given by

$$f_{rs} = f_{rs} + 1 \tag{16}$$

to count each time the corresponding P_{rs} is reached. Thus, f_{rs} gives a measure of the capability of a manipulator to reach workspace points in several ways. This can be considered a measure of repeatability and dexterity of a manipulator. Indeed, a synthetic measure can be proposed as the average D_z over the sum of all the values of the entries frs for each cross-section.

In addition, the proposed formulation is useful for a numerical evaluation of the position workspace by computing the cross-sections areas A_z as

$$A_z = \sum_{r=1}^{r_{max}} \sum_{s=1}^{s_{max}} (P_{rs} \, \Delta x \, \Delta y) \tag{17}$$

and finally the workspace volume V can be computed as

$$V = \sum_{z=z_{min}}^{z=z_{max}} A_z \, \Delta_z \tag{18}$$

An average D_{tot} over the sum of all the values of the D_z can give a synthetic measure for repeatability and dexterity capability of a given manipulator.

Similarly, a numerical evaluation of orientation workspace can be carried out by using the formulation of Eqs. (14) to (18) in order to compute the corresponding performance measures cross-sections areas $A\varphi$, the orientation workspace volume $V\varphi$, the average $D\varphi$ over the sum of all the values of the entries f_{rs} for each cross-section, and the average $D\varphi_{tot}$ over the sum of all the values of the $D\varphi$.

Of course, one can use Eqs. (14) to (17) in order to evaluate any cross-section by properly adapting the formulation to the scanning cross-section plane and intervals.

4. A WORKSPACE CHARACTERIZATION AND EVALUATION OF ECLIPSE ROBOT ARCHITECTURE

The basic workspace characteristics of the Eclipse robot architecture have been determined numerically by using the proposed procedure. Results are shown in Figs. 6 to 18 and Tables II to V.

In particular, the computation has been carried out by considering the nature and generation of workspace due to specific mobility range of the actuated joints as given from the mechanical design of the built prototype of Fig. 2.

The Workspace can be considered as the union of unit volumes, which have the same manifold geometry. The union set can be obtained by translating the unit volume along the vertical direction in agreement with the stroke of the vertical prismatic joints. Therefore, the basic workspace characteristics are related to the manifold of the unit workspace volume. The unit workspace volume can be obtained by computing the reachable points when the vertical prismatic guides are fixed at any value. The workspace can be evaluated for positioning capability as a Position Workspace and for orientating capability as an Orientation Workspace.

Specifically, the Orientation Workspace of an Eclipse robot can be characterized by the orientation capability of the points of the unit orientation workspace volume.

The proposed numerical algorithm does not consider the current mobility of the joints. In particular, the current motion of the joints on the vertical guides gives additional straight-line segments for each point of the computed unit position workspace; current motion of the joints on the planar circular guide gives additional circles for each point of the computed unit position workspace. Thus, the Position Workspace will have a cylindrical shaped volume with a bulk circle cross-section.

The current mobility of the sliding joints in the vertical and circular guides do not affect the orientation capability of the Eclipse robot, since the mobile plate moves with a translational motion, which keeps unchanged the orientation of the mobile plate.

For computational convenience the conditions $s_1 = s_2 = s_3 = 0$ have been assumed and Figs. 6 to 12 have been obtained for the unit workspace volume. In the case of the analysis of the theoretical capability with no constraints on joints mobility the number of computed reachable points

Table II. Numerical values of the cross-section areas and corresponding maxima of the reach frequency matrices for the nine cross-sections used in the evaluation of Fig.11 a) for the unit position workspace starting with k=1 for z =z_{min}.

k	1	2	3	4	5	6	7	8	9
Area (mm^2)	731,482	731,842	658,333	1,097,223	1,097,223	950,926	877,778	731,481	658,333
Max freq	13,490	6,599	5,009	4,144	4,556	5,068	6,718	13,647	7,796

Table III. Numerical values of the cross-section areas and corresponding maxima of the reach frequency matrices for the nine cross-sections used in the evaluation of Fig.11 b) for the unit position workspace starting with k=1 for z =z_{min}.

k	1	2	3	4	5	6	7	8	9
Area (mm^2)	29,400	31,360	30,053	27,440	24,826	24,826	25,480	1,306	1,306
Max freq	357	1,063	2,301	2,163	1,909	1,850	1,349	31	23

Table IV. Numerical values of the cross-section areas and corresponding maxima of the reach frequency matrices for the nine cross-sections used in the evaluation of Fig.12 a) for the unit position workspace starting with k=1 for $\varphi = \varphi_{min}$.

k	1	2	3	4	5	6	7	8	9
Area (deg^2)	39,866	50,599	30,666	15,333	21,466	30,666	45,999	27,599	21,467
Max freq	14,032	7,455	17,025	24,887	20,389	14,302	7,521	6,572	9,297

Table V. Numerical values of the cross-section areas and corresponding maxima of the reach frequency matrices for the nine cross-sections used in the evaluation of Fig.12 b) for the unit position workspace starting with k=1 for $\varphi = \varphi_{min}$.

k	1	2	3	4	5	6	7	8	9
Area (deg^2)	15,555	24,888	7,777	6,222	9,333	12,444	23,333	12,444	12,444
Max freq	2,059	2,201	10,623	9,581	5,043	3,870	2,200	4,169	4,485

has been 197,379 when the scanning process has been carried out with discretization values $\Delta\alpha_1 = \Delta\alpha_2 = \Delta\alpha_3 = 10$ deg. and $\Delta\beta_1 = 15$ deg. When constraints for joint mobility have been taken into account, the number of feasible computed points has been reduced to 96,196.

Figure 6 gives the unit Position Workspace. It is possible to see symmetry properties, mainly from the Workspace cross-sections of Fig. 7. But the Position Workspace volume is strongly reduced when joint constraints are taken into account, as it can be seen from a comparison between the plots a) and b) of Figs. 6 and 7.

Similar observations can be deduced for the Unit Orientation Workspace from results shown in Figs. 8 and 9. It is remarkable to find a large motion range in orientation

although with a very peculiar shape in the reachable regions.

Figure 10 gives the workspace characteristics in terms of both position and orientation, so that one can determine for each given position or orientation the range of feasible orientations and positions, respectively.

The workspace capability has been better described by determining Figs. 11 and 12 for the corresponding cross-sections of the Position and Orientation Unit Workspaces, respectively, by giving also a comparison between the cases with no constraints and mobility constraints for the joints. It is remarkable to find a strong reduction of the values of the repeatability measure, although the shape of the plots is maintained in most of the cases. The numerical character-
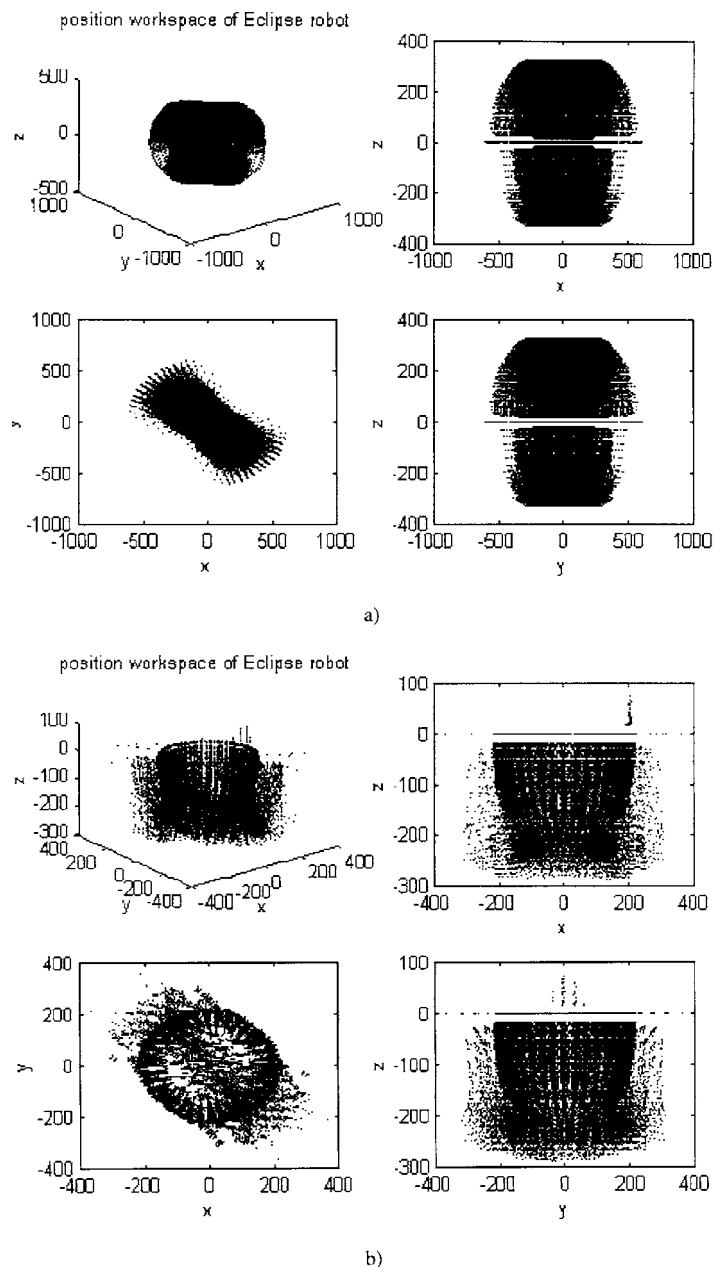
Fig. 6. Position Unit Workspace of an Eclipse robot as a 3D view and projections onto Cartesian planes: a) theoretical results; b) when mobility constraints for the joints are considered.
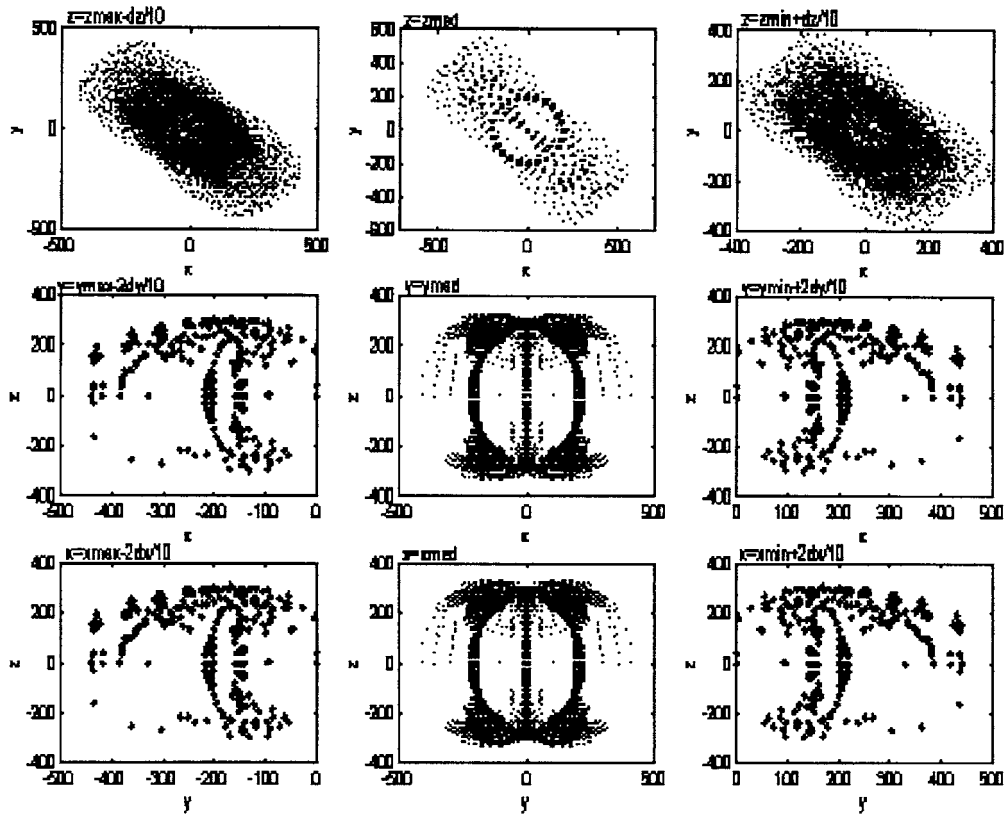
a)
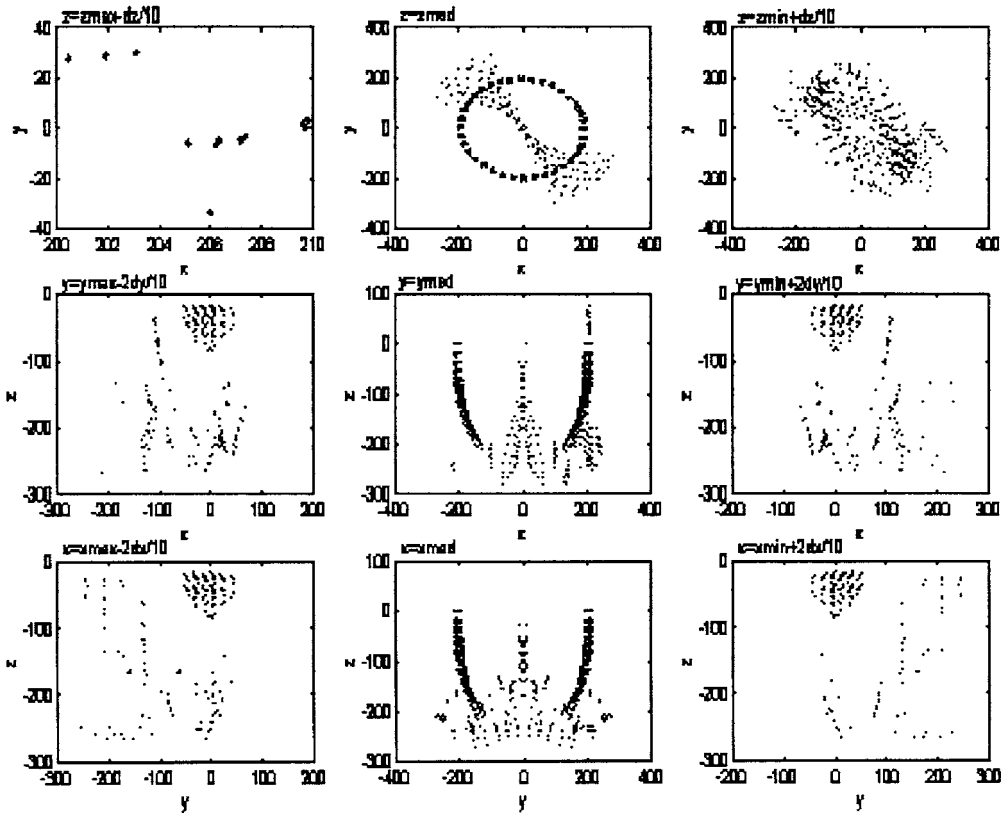
b)

Fig. 7. Cross-sections of the Position Unit Workspace of an Eclipse robot for scanning interval of 15 deg for α_{kj} and slice thick 5 mm: a) theoretical results; b) when mobility constraints for the joints are considered.

orientation workspace of Eclipse robot

a)

orientation workspace of Eclipse robot

b)
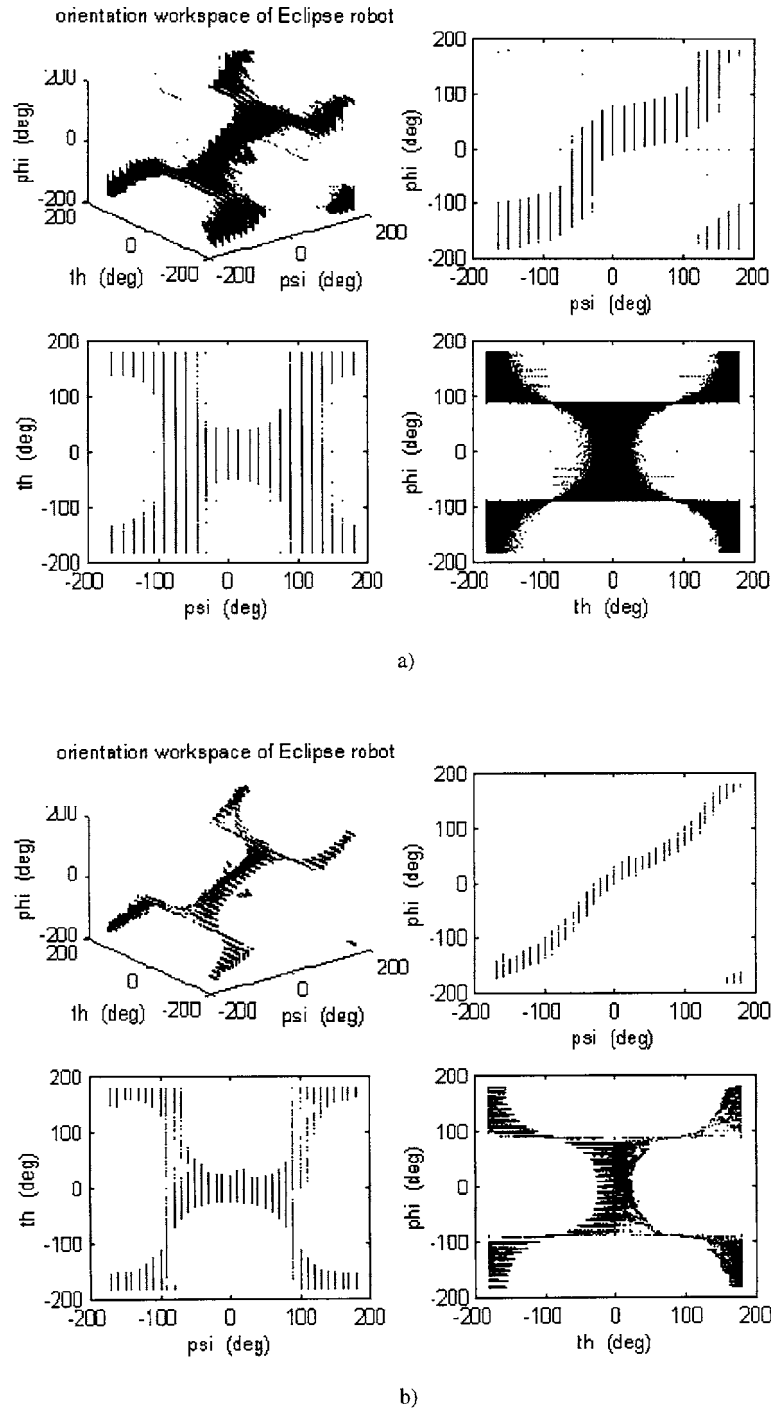
Fig. 8. Orientation Unit Workspace of an Eclipse robot: 3D view and projections onto Cartesian planes: a) theoretical results; b) when mobility constraints for the joints are considered.

ization has been better shown in Tables II, III, IV, and V by giving also the value of the cross-section areas.

The constraints on the sliding joints have given a considerable reduction of the workspace capability in term of position mainly along the Z-axis, but not in term of orientation, as observable from Figs. 6, and 8, 7 and 9.

A symmetry of workspace volumes is also found for both theoretical and constrained workspace determinations.

For the computation of the workspaces of the Eclipse prototype of Fig. 2 the discretization of the mobility of the vertical sliding joints has been assumed as

$\Delta s_1 = \Delta s_2 = 100$ mm and $\Delta s_3 = 150$ mm with $\Delta \alpha_1 = \delta \alpha_2 = \Delta \sigma_3 = 10$ deg. and $\Delta \beta_1 = 15$ deg. so that the total workspace has been computed by using only three Unit Workspaces, namely the top one, the bottom one and the middle one, in order to determine the extreme reach capability of the Eclipse robot prototype. Results are shown in Figs. 13 to 18 and Tables VI and VII.

It is worth noting the enlarged shape of the Position workspace along Z-axis, but the unchanged Orientation Workspace with respect to the corresponding Unit Workspaces. Figures 13 to 18 have been reported not only to give

a)

b)
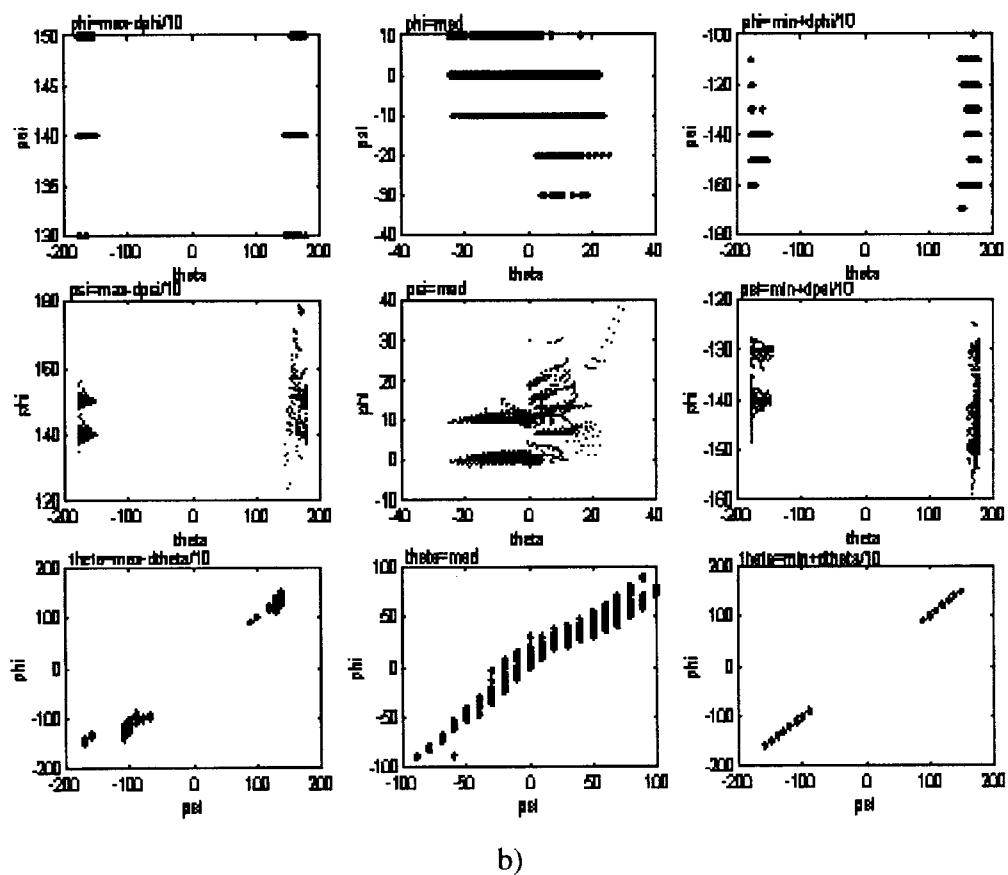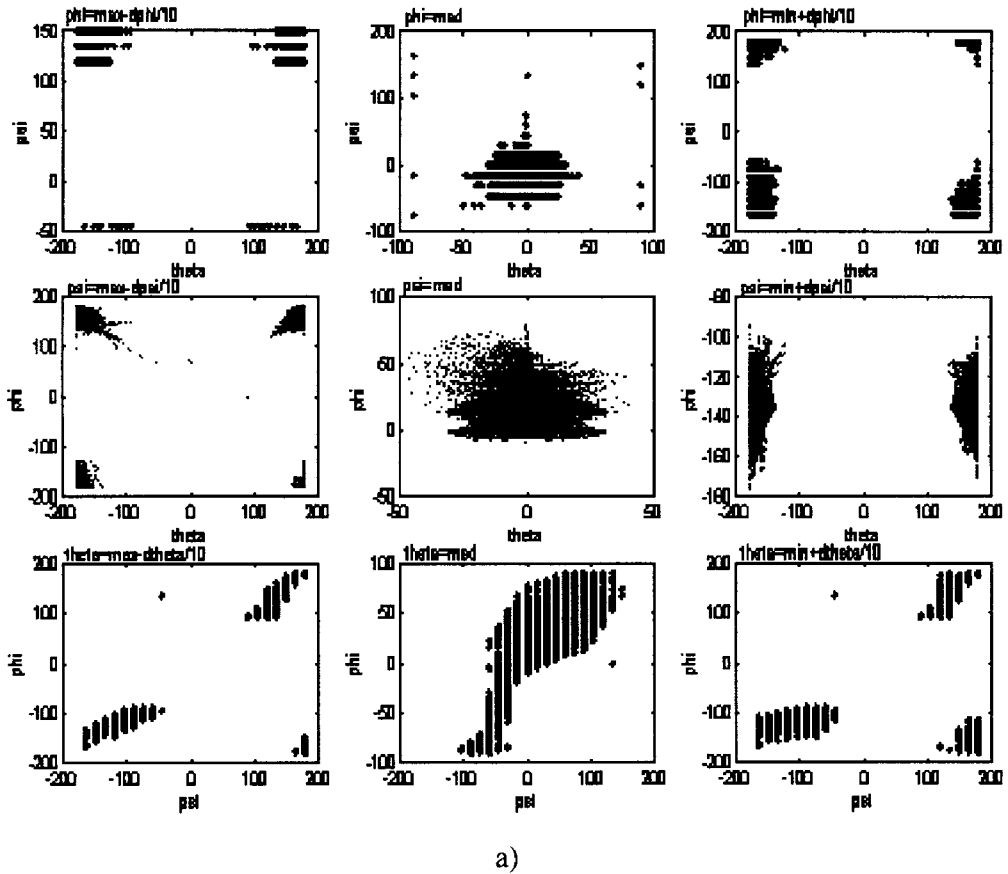
Fig. 9. Cross-sections of the Position Unit Workspace of an Eclipse robot for scanning interval of 15 deg for α_{kj} and slice thick 5 deg.: a) theoretical results; b) when mobility constraints for the joints are considered.
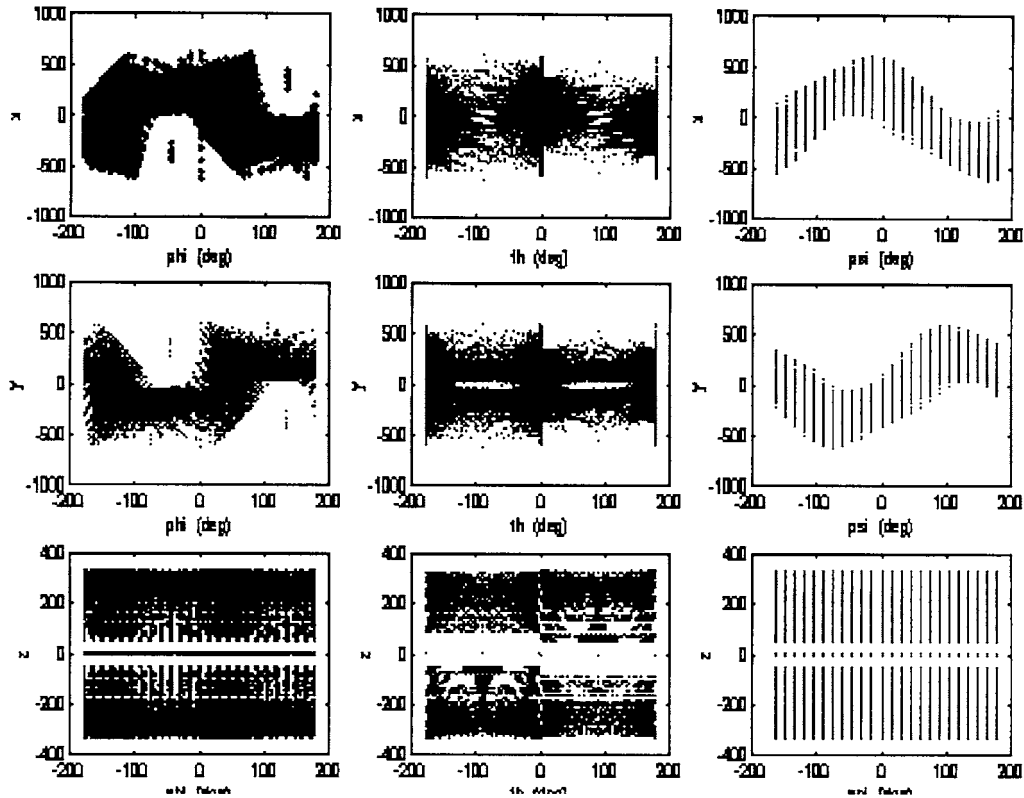
Fig. 10. Unit Workspace of an Eclipse robot, when mobility constraints for the joints are not considered: X-coordinate of H versus orientation angles; Y-coordinate of H versus orientation angles; Z-coordinate of H versus orientation angles.

the final result of the workspace determination for the Eclipse robot prototype of Fig. 2, but mainly to show the relevant significance of the Unit Workspace values for characterizing the workspace of Eclipse robots.

5. CONCLUSIONS

Workspace performances are of basic significance for manipulator applications. The Eclipse parallel architecture is a novel parallel manipulator conceived at the National

Table VI. Numerical values of the cross-section areas and corresponding maxima of the reach frequency matrices for the nine cross-sections used in the evaluation of Fig. 17 for the position workspace starting of Fig. 13 with k=1 for $z=z_{min}$.

k	1	2	3	4	5	6	7	8	9
Area (mm²)	39,811	42,724	47,579	49,521	46,666	48,550	33,985	8,739	3,884
Max freq	411	4,459	5,715	6,692	3,907	1,665	422	91	13

Table VII. Numerical values of the cross-section areas and corresponding maxima of the reach frequency matrices for the nine cross-sections used in the evaluation of Fig.18 for the position workspace starting of Fig.14 with k=1 for $\varphi=\varphi_{min}$.

k	1	2	3	4	5	6	7	8	9
Area (deg²)	35,266	29,133	18,399	15,333	21,466	26,066	26,066	18,399	19,933
Max freq	4,092	9,595	10,910	10,990	7,240	4,460	11,788	4,996	5,708

a)

b)
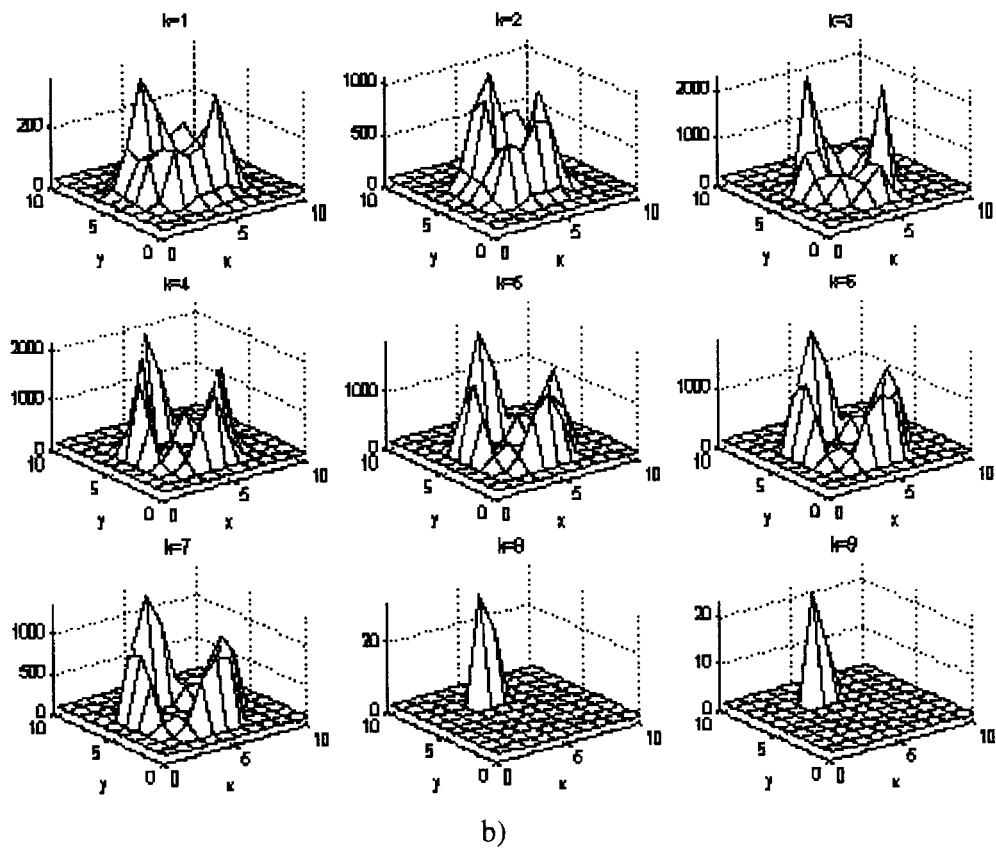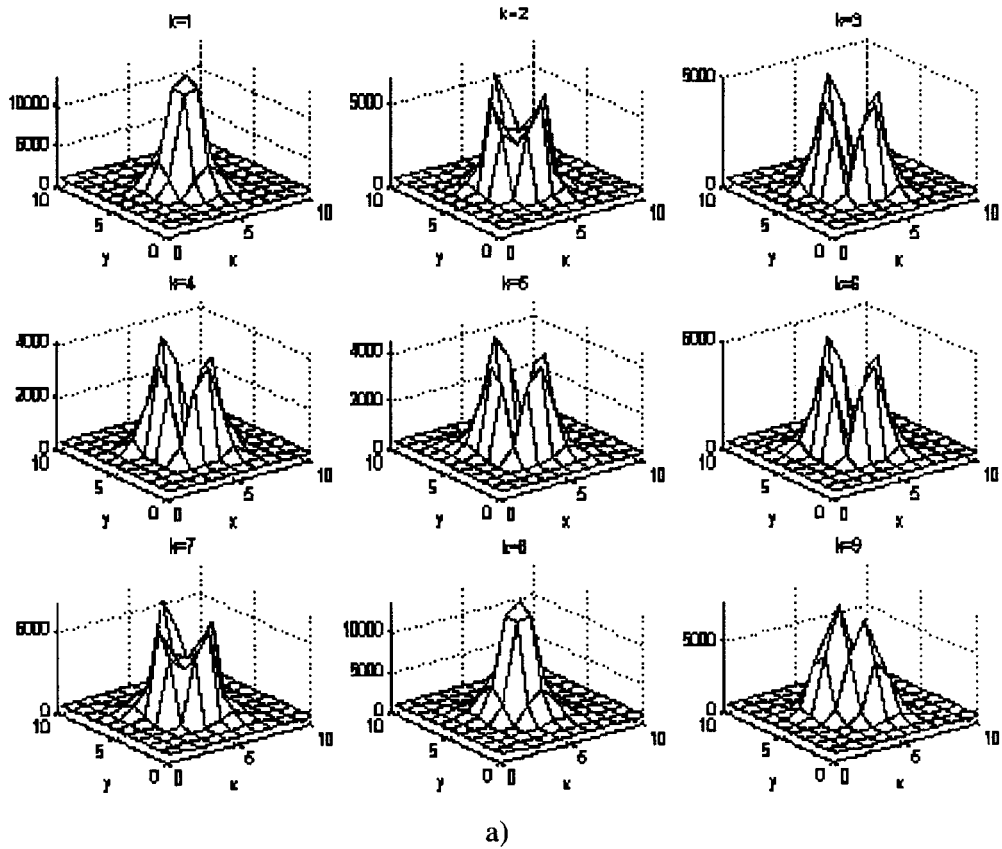
Fig. 11. Mapping of the position repeatability measure in the nine cross-sections of Fig. 6 along Z-axis: a) theoretical results; b) when mobility constraints for the joints are considered.
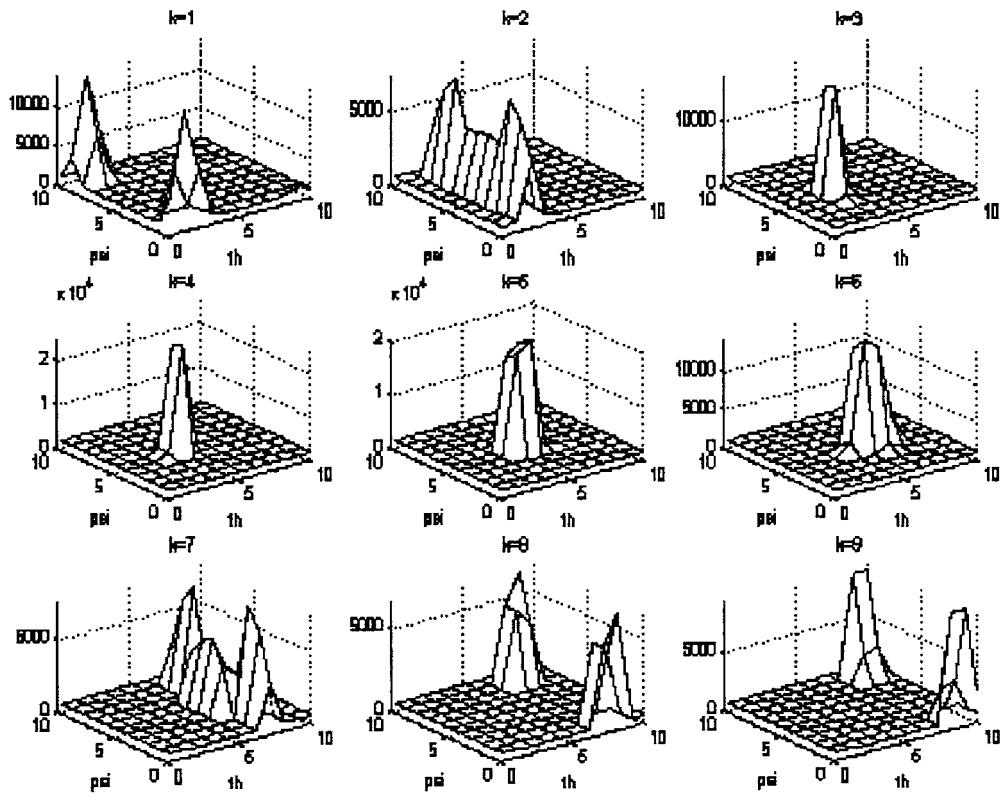
a)
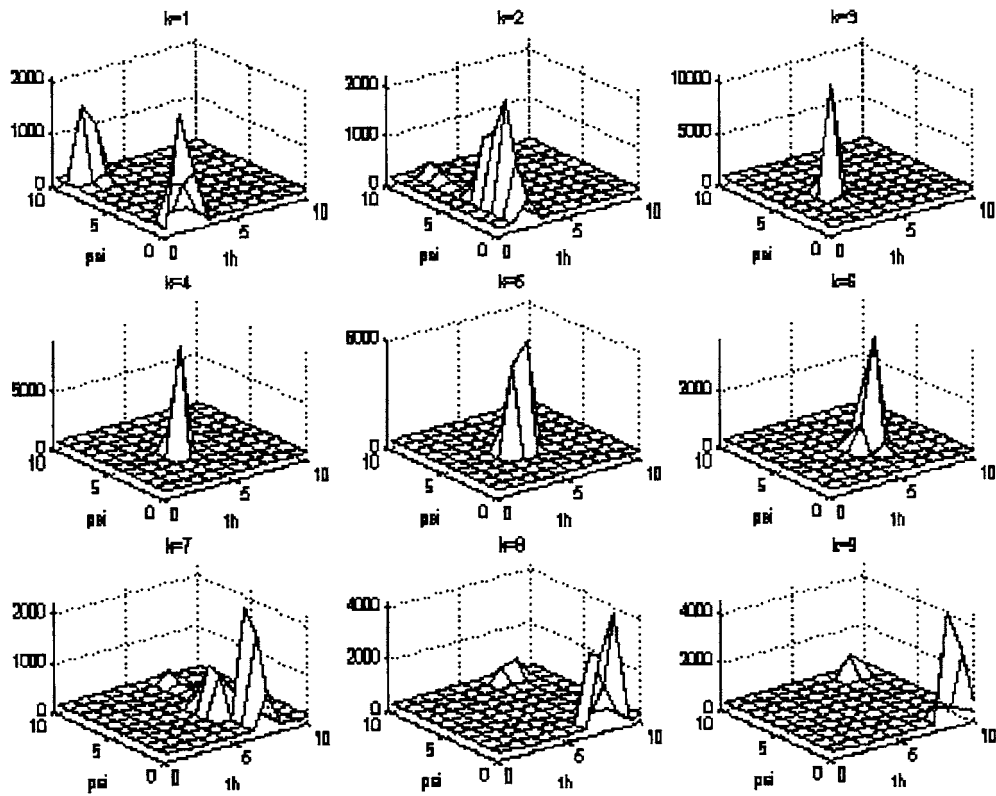
b)

Fig. 12. Mapping of the orientation repeatability measure in the nine cross-sections of Fig. 7 along φ-axis: a) theoretical results; b) when mobility constraints for the joints are considered.
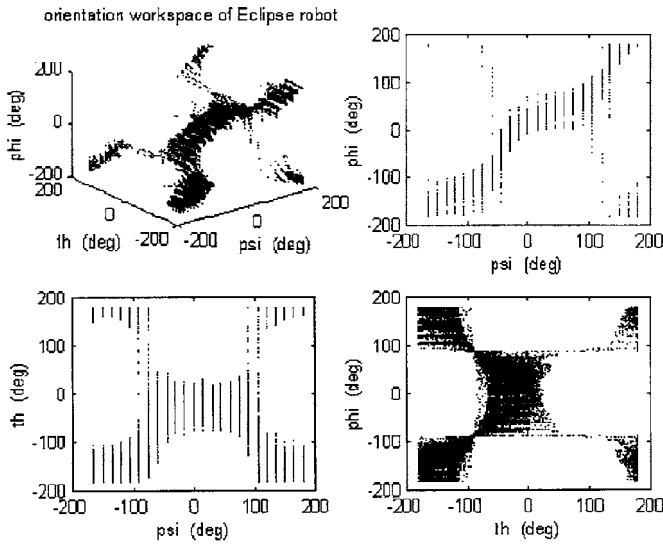
Fig. 13. Position Workspace of an Eclipse robot prototype of Fig.2: 3D view and projections onto Cartesian planes when mobility constraints for the joints are considered.
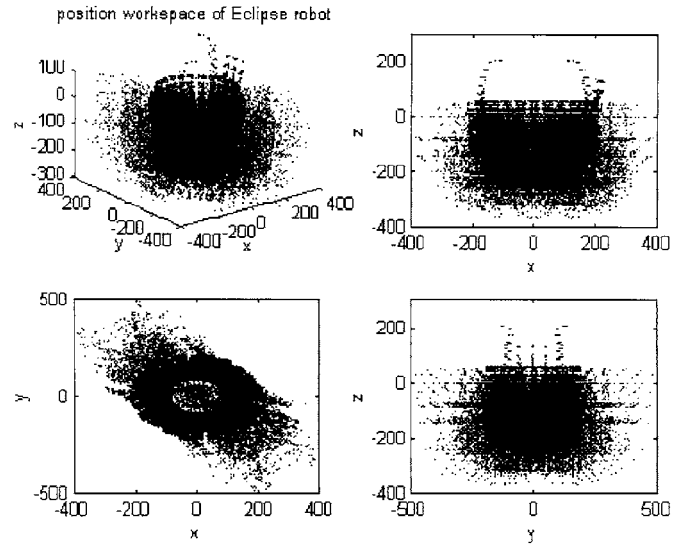
Fig. 14. Orientation Workspace of an Eclipse robot prototype of Fig.2: 3D view and projections onto Cartesian planes when mobility constraints for the joints are considered.

University of Seoul, Korea. Collaboration with the Laboratory of Robotics and Mechatronics in Cassino, (Italy) has been carried out in order to investigate the workspace characteristics of the Eclipse robot architecture.

In this paper we have reported a suitable numerical procedure that has been developed *ad-hoc* for the determining workspace characteristics of the Eclipse robot

architecture. The numerical procedure has been based on a formulation of both the specific parallel architecture and RSSR sub-mechanism of an Eclipse robot.

Results of a workspace characterization of Eclipse robot and its prototype have been reported, showing the shape and size of the reachable unit volume for orientation and position capability.
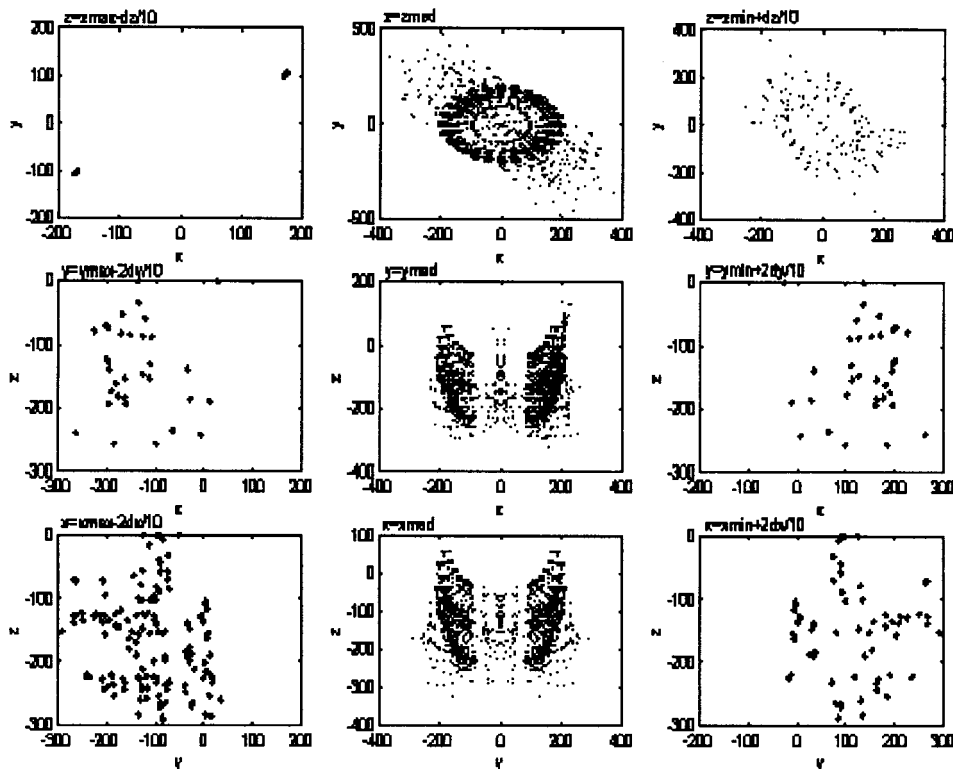
Fig. 15. Cross-sections of the Position Workspace of an Eclipse robot prototype of Fig.2 for scanning interval of 15 deg for α_{kj} 5 mm for s_{kj} and slice thick 5 mm when mobility constraints for the joints are considered.
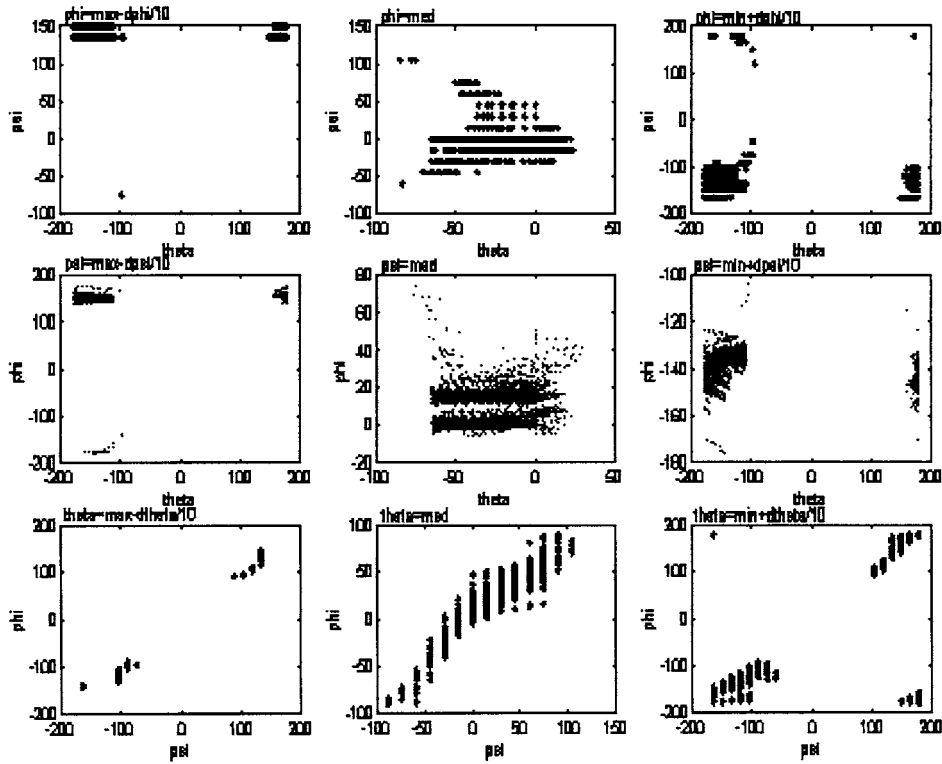
Fig. 16. Cross-sections of the Orientation Workspace of an Eclipse robot prototype of Fig. 2 for scanning interval of 15 deg for α_{kj} 5 mm for s_{kj} and slice thick 5 mm when mobility constraints for the joints are considered.
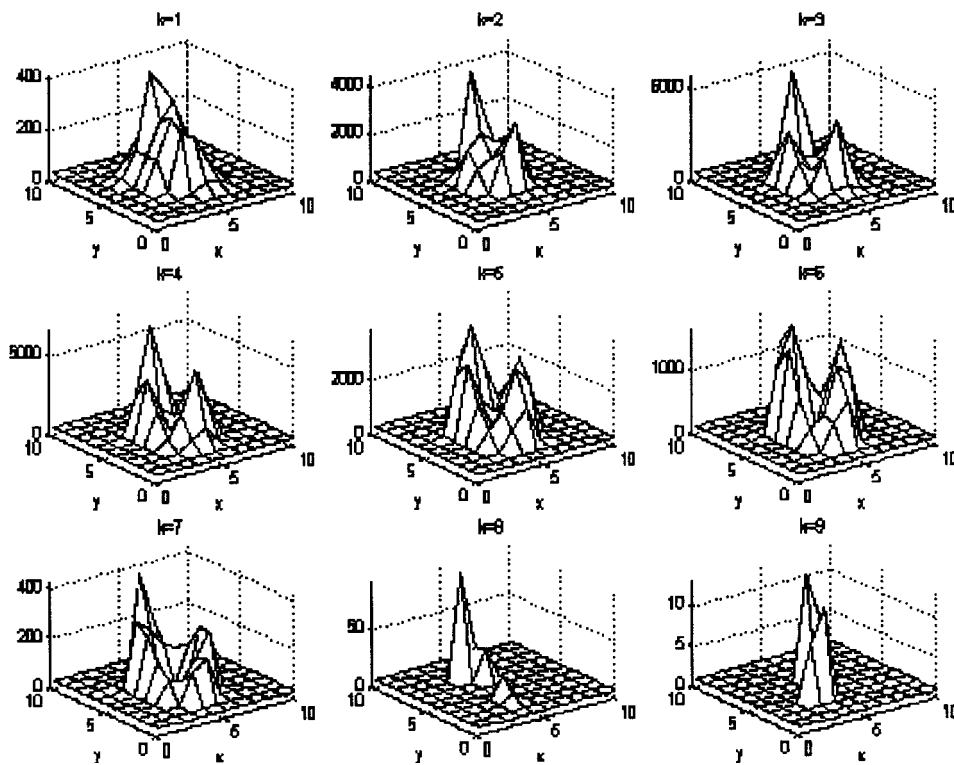
Fig. 17. Mapping of the position repeatability measure in the cross-sections along Z-axis for an Eclipse robot prototype of Fig. 2 when mobility constraints for the joints are considered.

Fig. 18. Mapping of the orientation repeatability measure in the cross-sections along φ-axis for an Eclipse robot prototype of Fig. 2 when mobility constraints for the joints are considered.

References
1. C. Gosselin, "Determination of the Workspace of 6-DOF Parallel Manipulators", *ASME Journal of Mechanical Design*, **112**, No. 3, 331–336 (1990).
2. J.-P. Merlet, "Designing a Parallel Manipulator for a Specific Workspace", *The International Journal of Robotic Research*, **16**, No. 4, 545–556 (1997).
3. M. Ceccarelli, "A New 3 dof Spatial Parallel Mechanism", *Mechanism and Machine Theory*, **32**, No. 8, 895–902 (1997).
4. J. Kim, F. C. Park, J. W. Kim, J. C. Hwang, "ECLIPSE: An Overactuated Parallel Mechanism for Rapid Machining", *Proc. Of ASME-IMECE Symposium on Machine Tools*, Anaheim, (1998) pp. 15–20.
5. F. C. Park, J. W. Kim, "Design and Integration Issues in a Parallel Mechanism-Based Rapid Prototyping System", *Proc. of 7th International Workshop on Robotics in Alpe-Adria-Danube Region RAAD'98*, Smolenice (1998) pp. 157–162.
6. M. Ceccarelli, F. C. Park, E. Ottaviano, J. Kim, "Workspace Analysis of the Eclipse Robot", *Proc. of 9th International Workshop on Robotics in Alpe-Adria-Danube Region RAAD2000*, Maribor (2000) pp. 269–274.